Icarus 264 (2016) 456–464

Contents lists available at ScienceDirect

Icarus

journal homepage: www.journals.elsevier.com/icarus

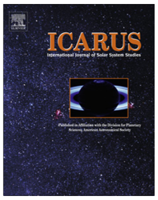

The solsticial pause on Mars: 1. A planetary wave reanalysis

Stephen R. Lewis [a,*], David P. Mulholland [b,1], Peter L. Read [b], Luca Montabone [b], R. John Wilson [c], Michael D. Smith [d]

[a] Department of Physical Sciences, The Open University, Walton Hall, Milton Keynes MK7 6AA, UK
[b] Atmospheric, Oceanic & Planetary Physics, University of Oxford, Clarendon Laboratory, Parks Road, Oxford OX1 3PU, UK
[c] Geophysical Fluid Dynamics Laboratory, National Oceanic and Atmospheric Administration, Princeton, NJ 08540-6649, USA
[d] NASA Goddard Space Flight Center, Greenbelt, MD 20771, USA

ARTICLE INFO

Article history:
Received 16 April 2015
Revised 18 August 2015
Accepted 31 August 2015
Available online 15 September 2015

Keywords:
Mars, atmosphere
Mars, climate
Atmospheres, dynamics

ABSTRACT

Large-scale planetary waves are diagnosed from an analysis of profiles retrieved from the Thermal Emission Spectrometer aboard the Mars Global Surveyor spacecraft during its scientific mapping phase. The analysis is conducted by assimilating thermal profiles and total dust opacity retrievals into a Mars global circulation model. Transient waves are largest throughout the northern hemisphere autumn, winter and spring period and almost absent during the summer. The southern hemisphere exhibits generally weaker transient wave behaviour. A striking feature of the low-altitude transient waves in the analysis is that they show a broad subsidiary minimum in amplitude centred on the winter solstice, a period when the thermal contrast between the summer hemisphere and the winter pole is strongest and baroclinic wave activity might be expected to be strong. This behaviour, here called the 'solsticial pause,' is present in every year of the analysis. This strong pause is under-represented in many independent model experiments, which tend to produce relatively uniform baroclinic wave activity throughout the winter. This paper documents and diagnoses the transient wave solsticial pause found in the analysis; a companion paper investigates the origin of the phenomenon in a series of model experiments.

© 2015 The Authors. Published by Elsevier Inc. This is an open access article under the CC BY license (http://creativecommons.org/licenses/by/4.0/).

1. Introduction

Planetary wave activity has been observed in the martian winter polar and midlatitude regions in telescopic images and by spacecraft since NASA Mariner 9 and the Viking Landers (e.g. Ryan et al., 1978) and later by Mars Global Surveyor (MGS) (Wilson et al., 2002; Banfield et al., 2004; Hinson and Wang, 2010) and Mars Reconnaissance Orbiter (MRO) (Banfield et al., 2010) amongst others. Waves with periods of 2–7 sols and zonal wavenumbers $s = 1$–4 are typically the most prominent (Barnes, 1980), and amplitudes are much larger in the northern hemisphere (up to 20 K) than in the southern hemisphere (up to 3.5 K) (Banfield et al., 2004). While the largest scale $s = 1$ wave can extend several scale heights above the surface, waves with shorter wavelengths are more confined in the vertical. Several Mars global circulation models (MGCMs) are able to produce waves of broadly similar periods and wavenumbers to those observed (e.g. Barnes et al., 1993; Collins et al., 1996; Wilson et al., 2002).

Whilst wave activity is seen in the northern hemisphere from late summer through to spring, variation in the relative strengths of different zonal wavenumbers has been reported. Banfield et al. (2004) find that $s = 1$ waves dominate around winter solstice, while $s = 2$ and $s = 3$ waves are strongest during autumn and spring. This dominance of the vertically extended $s = 1$ wave at winter solstice ($L_S = 270°$) coincides with a minimum in eddy activity near the surface at this time, a phenomenon known as the 'solsticial pause' (Wang et al., 2005), perhaps first noticed by Barnes (1980) in Viking surface pressure data. This suppression is limited to the lowest 1–2 scale heights of the atmosphere, and transient temperature perturbations above this are seen to reach a maximum around winter solstice (Wang et al., 2005).

Such a suppression, through a reduction in surface windspeed variance and magnitude (Wang et al., 2003), is suspected to exert a strong control over dust lifting along the seasonal polar cap edge. The progression of frontal dust storm frequency in northern midlatitudes has been seen to display a double-peaked structure (Wang, 2007), with a significant reduction in all dust storm activity in the northern hemisphere observed in the later part of a record from $L_S = 170$–$270°$ in three Mars Years (Cantor, 2007). More recently, Guzewich et al. (2015) have identified clear minima at

---

* Corresponding author.
E-mail address: stephen.lewis@open.ac.uk (S.R. Lewis).

[1] Present address: Department of Meteorology, University of Reading, Harry Pitt Building, Reading RG6 6AL, UK.

http://dx.doi.org/10.1016/j.icarus.2015.08.039
0019-1035/© 2015 The Authors. Published by Elsevier Inc.
This is an open access article under the CC BY license (http://creativecommons.org/licenses/by/4.0/).

both solstices in their dust storm climatology based on MGS Mars Observer Camera (MOC) images.

Wang et al. (2013) showed that simulated travelling waves generated significant amounts of energy baroclinically near the surface before and after solstice, but that this generation was greatly reduced at solstice, while eddy kinetic energy was generated barotropically above 30 km throughout the autumn and winter period.

Solsticial minima in transient wave activity of varying amplitudes have been simulated by MGCMs, using prescribed dust distributions representing major dust storm conditions (Hourdin et al., 1995; Kuroda et al., 2007), with more typical prescribed dust loadings (Wilson et al., 2006; Wang et al., 2013; Kavulich et al., 2013), and in an interactive dust-lifting model (Basu et al., 2006). Outside of dust storm conditions, however, modelled reductions to near-surface waves in models have generally not been as dramatic as those observed in the martian atmosphere (e.g. Wang et al., 2005). The reasons for the development of these winter minima, and for their partial representation in MGCMs, have not been fully explored, particularly with regard to the fact that the phenomenon is not restricted to martian years which include a major dust storm (Wang et al., 2005).

This paper documents and diagnoses the transient wave solsticial pause found in a reanalysis (Lewis et al., 2007; Montabone et al., 2006, 2014) of three martian years of Thermal Emission Spectrometer (TES) data (Conrath et al., 2000; Smith et al., 2000; Smith, 2004) into a MGCM. Similar results are found in reanalyses of subsequent years using MCS data, but here we focus on the phenomenon in the most well validated period with data from a single instrument that demonstrates its repeatability in both years with and without a global dust storm. A companion paper (Mulholland et al., 2016) investigates the origin of the phenomenon in a series of independent MGCM experiments.

2. Model and data assimilation

The model used for this study is the UK version of the LMD MGCM developed through a collaboration between groups in France and the UK (Forget et al., 1999; Lewis et al., 1999). The UK version of the model uses a spectral solver for the primitive equations (Hoskins and Simmons, 1975), and employs a semi-Lagrangian advection scheme to transport dust, water vapour, water ice and other tracers (Newman et al., 2002), although tracer transport was not used for the assimilations presented in the present paper, and instead dust was assimilated and updated whenever new observations became available. This is in contrast to the independent model experiments presented in P2. The analyses described here were all carried out using a triangular spectral truncation at total wavenumber 31, corresponding to a $3.75^\circ \times 3.75^\circ$ dynamical grid for nonlinear products and a $5^\circ \times 5^\circ$ physical processes grid, with 25 levels in the vertical between the surface and roughly 100 km altitude.

Data assimilation was conducted using a modified form of the analysis correction scheme (Lorenc et al., 1991), as described in Lewis et al. (2007), using version 2 of the TES retrievals (Smith, 2004) for the scientific mapping period of almost three Mars years (MY) from MY24, $L_S = 141^\circ$ to MY27, $L_S = 72^\circ$ (with updated data and a slightly extended time period from an analysis presented in Montabone et al., 2006). Thermal profiles and total dust opacities from nadir retrievals were assimilated into the model, each centred on the time and place at which they were valid, and model output was stored at two-hourly intervals throughout this period for later analysis. The benefits of data assimilation are that the reanalysis combines information from past and present data and produces physically consistent variables when and where they are not observed. Wave behaviour, in particular, may then be diagnosed more easily using the regularly sampled data set than using the retrievals. All results presented in this paper are taken from this three-year reanalysis (Montabone et al., 2014).

3. The martian solsticial pause

We now describe the martian solsticial pause in wave activity, as represented in the reanalysis. The first subsection describes its temporal form and vertical structure, using longitudinally-averaged data. The following subsection describes the zonal structure of the eddies before during and after the solsticial pause. We then discuss the interannual variability in the phenomenon. Finally, we consider some possible other sources of observational evidence that support this analysis.

3.1. Temporal and vertical structure

Fig. 1 shows the root-mean-square (RMS) variance of atmospheric temperature, 2.5 km above the surface, illustrating clearly the solsticial pause in each of the three years of the assimilation of TES temperature data. The reanalysis data here and in related plots have been bandpass filtered to remove short-period waves, such as the diurnal tide, and any long-period, quasi-stationary waves, retaining only signals with a period within the range 1.5–30 sols. It can be seen that transient eddies are fairly weak (1–3 K) in the midlatitudes of each hemisphere at its winter solstice ($L_S = 90^\circ$ for the southern hemisphere and $L_S = 270^\circ$ for the northern hemisphere), but show peaks in activity either side of solstice, in late autumn and in early spring ($L_S = 0$–60°, 120–180° for the southern hemisphere, $L_S = 180$–240°, 300–360° for the northern hemisphere). This double-peaked structure, with a solsticial pause lasting for at least 60° of L_S in each hemisphere, emerges in each of the three years contained in the reanalysis, and is therefore not reliant on the occurrence of large dust storms (Smith, 2004) during specific periods. Variability in the timing of these events, however, does impart interannual variability to the near-surface eddies, particularly in the northern hemisphere, as discussed later (Section 3.3).

Transient eddy activity is generally stronger, by a factor of about two in terms of RMS air temperature, in the northern hemisphere than in the southern hemisphere: peak RMS values in the northern hemisphere are 7–8 K in each of the three years covered by the assimilation, while southern hemisphere values peak at around 4 K. The regions of peak RMS values in both hemispheres tend to form at higher latitude at the end of summer, move equatorward to mid-latitudes as winter progresses and then reduce in amplitude prior to the winter solstice. Once the eddies have grown again after the solstice, the region of greatest activity returns poleward until the eddies once again reduce in amplitude with the coming of spring. The latitude of the greatest eddy activity broadly follows the latitude of greatest thermal gradient near the surface, coinciding with the edge of the seasonal polar cap.

Fig. 2 illustrates the vertically limited nature of the solsticial pause, focusing on the northern hemisphere (50–70°N). While RMS temperature shows a clear minimum below 300 Pa around $L_S = 270^\circ$ every year, above this, between 100 Pa and 5 Pa, various maxima develop during the period $L_S = 180$–360°. Considerable interannual variability is evident: in MY25, a strong solsticial maximum in variance appears at this level; in the other two years, several shorter maxima form between $L_S \approx 200^\circ$ and $\approx 330^\circ$. These higher-altitude maxima form due to the large meridional temperature gradients that exist in this part of the atmosphere during autumn and winter, as a consequence of the middle atmosphere ‘polar warming’ (Kuroda et al., 2007; McCleese et al., 2008) (shown

Download English Version:

https://daneshyari.com/en/article/8135928

Download Persian Version:

https://daneshyari.com/article/8135928

Daneshyari.com